Geology and Geochemistry of the Metagabbros and Metavolcanics Rocks at El Igla Area Central Eastern Desert, Egypt

Aref M. Ahmed¹; Mahmoud M.A.M²; Farouk A. Soliman³; Ahmed S. Shalan²

¹ El Masrya for quarries Company ²Nuclear Materials Authority, Egypt ³Geology Department, Faculty of Science, Suez Canal University

Abstract

The Precambrian rocks of El Igla area, Central Eastern Desert, Egypt are consisting of metagabbros and metavolcanics cutting by syn-tectonic granites. El Igla metagabbros occurring as small to big outcrops, they are medium to coarse-grained and greenish grey to pale green in color, composed. They are showing ophitic to subophitic texture with calic pyroxenes and plagioclase as well as amphibole and pockets of hornblende as the major components. The alteration of El Igla metagabbros led to formation pyroxene, amphibole and actinolite. El Igla metavolcanics are exposed and comprise a heterogeneous of grey to green assemblages. They are coarse to medium grained and they are frequently interleaved with variably altered ultramafics (serpentinites) in the form of wedges and slices, with sharp tectonic contacts. El Igla metavolcanics are classified into meta-andesite, meta-basalt and meta-dacite rocks. Meta-andesite is composed essentially of plagioclase, hornblende and pseudomorphs chlorite. Accessory and secondary minerals are iron oxides, calcite, epidote and interstitial quartz. Meta-basalt is mainly composed of micro-phenocrysts of plagioclase, pyroxene and quartz set in a fine-grained groundmass exhibiting intersertal texture. Meta-Dacite is composed predominantly of plagioclase, quartz and biotite. They have a fine grained aphanitic to porphyritic texture.

The original magma of El Igla metagabbros was primitive and tholeititc to calc-alkaline in nature. They are fall in MORB type field and formed as a result of partial melting of mantle spinel peridotite that has been metasomatized by fluids dehydrated from a subducted slab. They are characterized by relatively parallel REE patterns with depletion of heavy rare earth elements ($\Sigma HREE = 7.91$) and enrichment in light rare earth elements (LREE = 49.79) with [(La/Yb)n = 1.17 - 2.06].

In El Igla metavolcanics, some major elements have wide compositional range of MgO (4.2-8.8 wt%) and MnO (0.11-0.18 wt%) with narrow compositional range of SiO₂ (49.3–52.1wt%), suggesting diverse protolith. The La/Sc ratios (0.03-6.57 with an average 0.97 ppm), the ratios of Y/Nb, and Nb/Y fall in the range between 1.91-15.63ppm with an average 5.90ppm and 0.06 – 0.53 ppm with an average 0.27ppm, respectively. The Nb/Y and La/Sc ratios are mostly < 1.0 and La/Y ratio is ranged from (0.05-0.56) with an average 0.22), implying possible approach to calc-alkaline and alkaline affinities with island arc setting.

Keyword: El Igla, Metagabbros, Metavolcanics, Geochemistry, Calc-alkaline, Central Eastern Desert

Date of Submission: 09-11-2025 Date of Acceptance: 21-11-2025

I. Introduction

The Egyptian gabbroic rocks are widely distributed in all tectonic environments from ophiolitic to continental settings [1, 2, 3]. Based on chronologic data, field relations, and tectonic settings, four groups of gabbroic rocks are distinguished [2]: (a) ophiolitic metagabbro, (b) island arc intrusive metagabbro–diorite complex, (c) intrusive fresh gabbros±ultramafic associations, and (d) gabbroic rocks associated with Phanerozoic ring complexes. In the Egyptian basement sequence, the gabbroic rocks post-date the calc–alkaline older granitoids and pre-date the calc–alkaline younger granitoids [4, 5, 6].

The Pan-African basement history of Wadi Abu Ghusun-Wadi Chatter district began with the arc volcanics (Ranga metavolcanics) passing through arc continent collision accompanied by the distribution of the oceanic lithosphere flooring the volcanic-arc and overthrusting of an oceanic slice (Atshan ophiolitic metabasalts) followed by emplacement of the Mahara and Abu Ghalaga metagabbros-diorite complexes [7].

The aim of the present paper is to shed more light on the geology and geochemical characteristics of El Igla metagabbros and metavolcanics.. El Igla area is located in the Central Eastern Desert of Egypt.

II. Location of the Study Area

El Igla area is located in the central Eastern Desert between longitudes 34° 42` 54" E and 34° 39` 54" E and latitudes 25° 08` 06" N and 25° 03` 54" N. It is easily accessible through Marsa Alam-Idfu asphaltic road at the entrance about 19km west of Marsa Alam city with track about 12km (Fig. 1A).

III. Geologic Setting and Petrography

The Precambrian basement rocks exposed in El Igla area represent a part of the Pan–African belt of the Arabian Nubian Shield [8]. El Igla area has a moderately to low topographic features.

El Igla area was studied in detailed and mapped on the scale 1:50,000 (Fig. 1B) using aerial photographs scale 1:40,000, photomosaic scale 1:50,000 and Landsat image scale 1:100,000.

3.1- Geology and Petrography of El Igla Metagabbros

El Igla metagabbros are found from small to big outcrops (Fig. 2) on the east and west side of the mapped area (Fig. 1B). They are medium to coarse-grained and greenish grey to pale green in color (Fig. 3). They form low and moderate relief and composed of plagioclase and amphibole as well as contain pockets of hornblende. The ophiolitic metagabbros are found as small fragments and blocks associated with serpentinites.

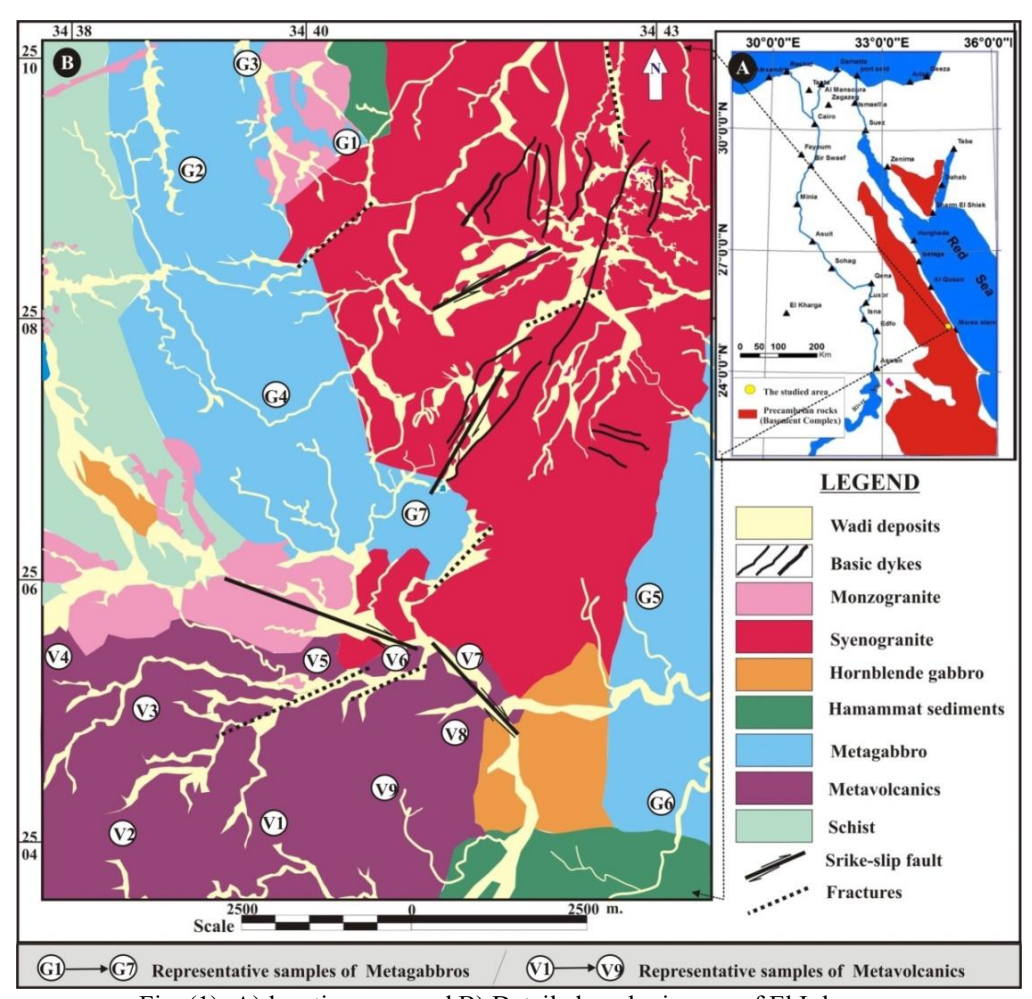


Fig. (1): A) location map and B) Detailed geologic map of El Igla area, Central Eastern Desert, Egypt





Fig. (2): The outcrop of El Igla metagabbros, Central Eastern Desert

Fig. (3): Greenish grey to pale green metagabbros at El Igla area

Petrographically, El Igla metagabbros are medium-sized grain and exhibit a hypidiomorphic texture. They are constituents of hornblende, plagioclase, calcic pyroxene, biotite and quartz. The accessory and secondary phases are magnetite, ilmenite, apatite, chlorite, epidote, iron oxides, actinolite and opaques.

Hornblende occurs either as subhedral to euhedral prismatic crystals, ranging in size from 0.2 to 0.6mm in width and from 0.5 to 1.0mm in length, sometimes, they show ophitic to subophitic texture (Fig. 4A), or as alteration products of olivine (Fig. 4B). It is slightly altered to chlorite and epidote along its cleavages. In some samples the hornblende partially serpentinized composed mainly of actinolite, chrysotile and antigorite associating carbonate. Actinolite occurs as fibrous aggregates showing faint pleochroic colors. Chrysotile is present as pale green foliated crystals associating talc (Fig. 4C). Antigorite is the main constituent occurring as platy crystals with colorless to gray colors and low relief. It occurs as aggregates of associated with carbonate (Fig. 4D).

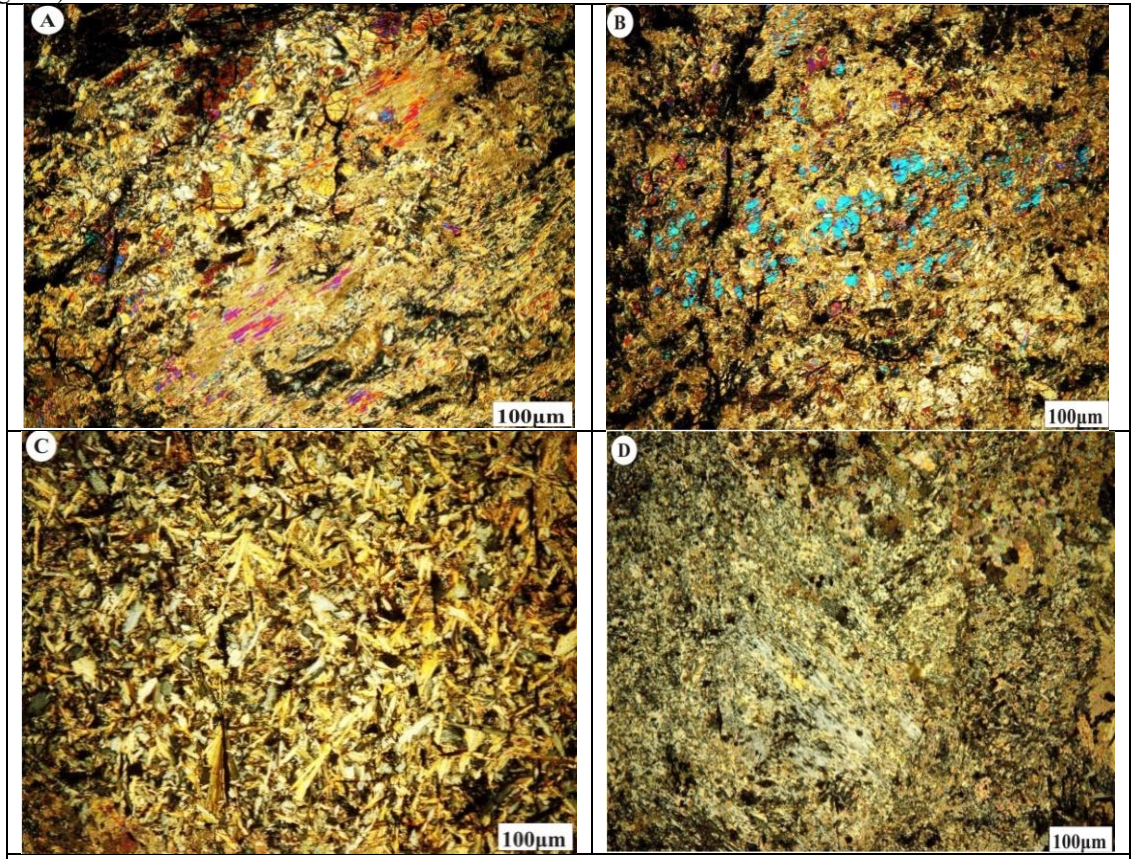


Fig. (4): Photomicrographs of El Igla Metagabbros showing; A) Hornblende crystals association with olivine and carbonate, notice ophitic to subophitic texture, B) Olivine crystals altered to hornblende, C) Fibrous crystals of actinolite and chrysotile, D) Fibrous crystals of antigorite associating carbonate.

3.2- Geology and Petrography of El Igla Metavolcanics

El Igla metavolcanics are exposed and comprise a heterogeneous of grey to green assemblage. They are coarse to medium grained and are abundant in southern parts of the mapped area (Fig. 1B). El Igla metavolcanics are frequently interleaved with variably altered ultramafics (serpentinites) in the form of wedges and slices, with sharp tectonic contacts (Fig. 5). Serpentinites locally contain patches of magnesite. Metavolcanics are intruded by monzogranite (Fig. 6).

Petrographically, El Igla metavolcanics classified into meta-andesite, meta-basalt and meta-dacite rocks. **Meta-andesite** rocks are composed essentially of plagioclase, hornblende and pseudomorphs chlorite. The accessory and secondary minerals are iron oxides, calcite, epidote and interstitial quartz.

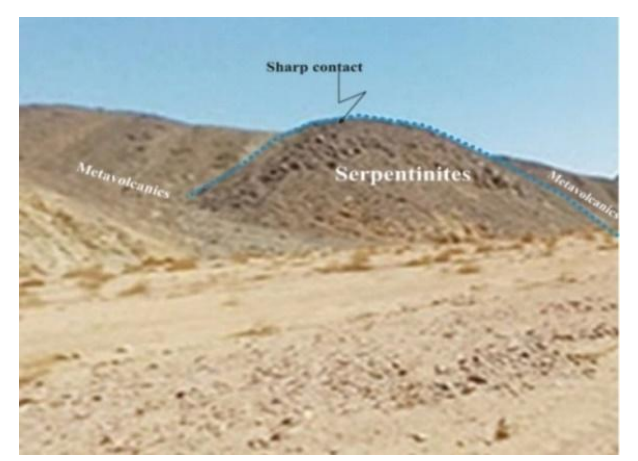


Fig. (5): Sharp contact between metavolcanics and serpentinite rocks at El Igla area.



Fig. (6): Metavolcanics intrude by monzogranite rocks at El Igla area.

Plagioclase megacrysts vary from 1.2 to 2.2mm long and from 0.4mm to 0.7mm width. They have andesine and labradorite compositions (An. 34-54). Zoning is quite common and twinning is according to albite and albite carlsbad laws. 1.2 to 2.2mm long and from 0.4mm to 0.7mm width. They have andesine and labradorite compositions (An. 34-54). Zoning is quite common and twinning is according to albite and albite carlsbad laws. Plagioclase phenocrysts show partial to complete cloudness due to alteration and associated with chlorite of penninite type (Fig. 7A). They usually elongate euhedral to subhedral crystals. Plagioclase of the groundmass form lathiform crystals (0.2 to 0.5mm long and up to 0.2mm width). It's usually andesine in composition (An. 36-40) and commonly altered. **Hornblende** is restricted to groundmass attaining 0.4mm long and showing completely altered to chlorite. **Carbonates** are always present in the form of patches or veinlets, associated with epidote, iron oxides, and sericite (Fig. 7B).

Meta-basalt rocks are mainly composed of micro-phenocrysts of plagioclase, pyroxene and quartz set in a fine-grained groundmass exhibiting intersertal texture (Fig. 7C). The groundmass of meta-basalt is formed of plagioclase, hornblende and quartz. Calcite, epidoten, chlorite and opaques are secondary minerals. **Plagioclase** (An. 25-40) occurs as subhedral blasto-porphyrites, up to 3.0mm long and dense aggregates in the groundmass. It is highly cracked, saussuritized and usually corroded by the quartz. **Pyroxene** shows fine euhedral to subhedral crystals varying from 0.3 to 4.0mm in length and from 0.2 to 0.5mm in width. It is highly altered, fine flakes and including plagioclase forming subophitic texture (Fig. 7D).

Meta-Dacite rocks are composed predominantly of plagioclase, quartz and biotite. They have a fine grained aphanitic to porphyritic texture. *Plagioclase* occurs as anhedral to subhedral blocky phenocrysts up to 3.0 mm long and dense aggregates in the groundmass. It is highly cracked and usually saussuritized (Fig. 7E). Plagioclase is corroded by secondary quartz and sometimes shows wavy extinction due to strain. *Quartz* appears as rounded and corroded phenocrysts or as an element of the groundmass (Fig. 6F). The groundmass is composed essentially of cryptocrystalline aggregates of quartz, plagioclase, hornblende, chlorite, epidote and opaques.

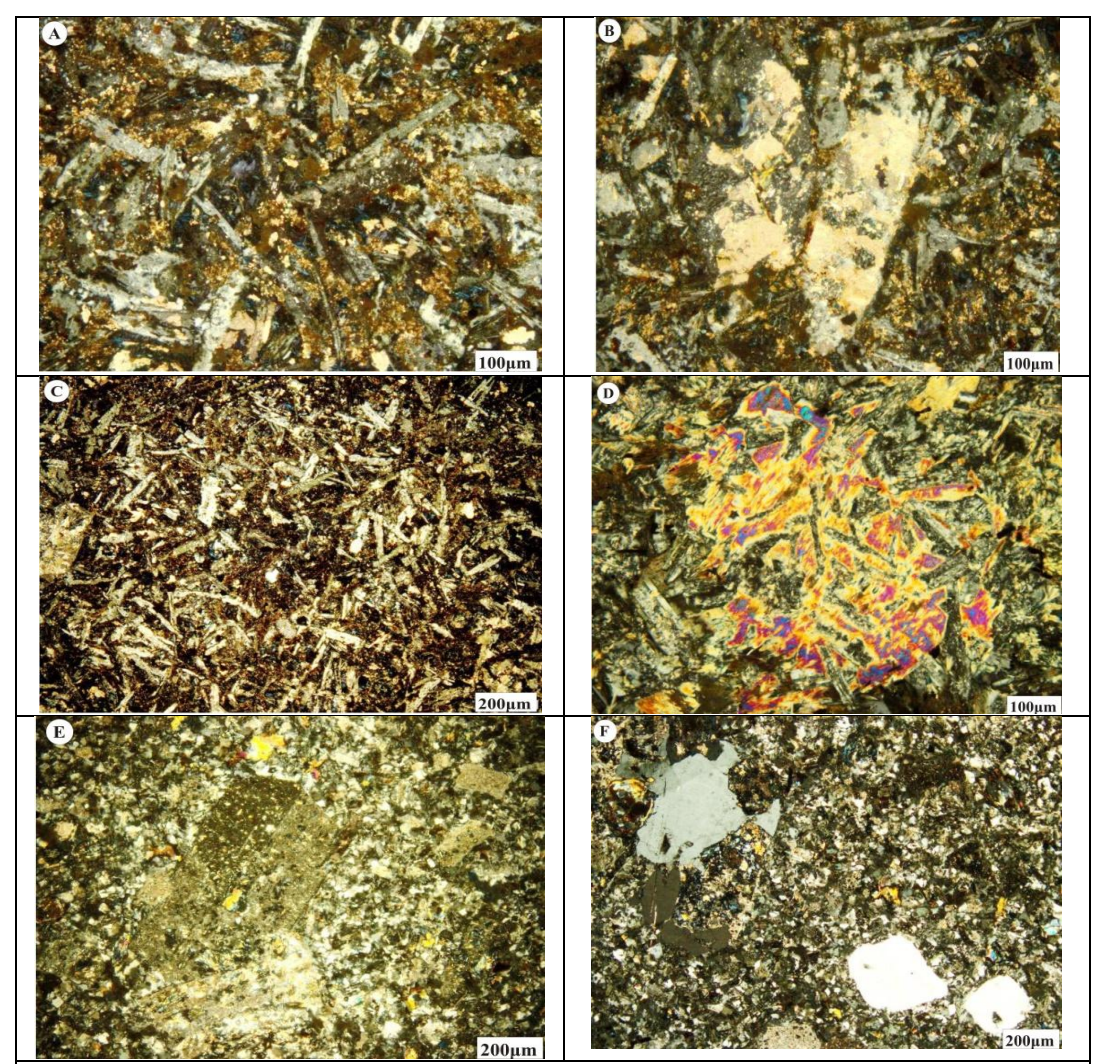


Fig. (7): Photomicrographs in El Igla meta-andesite and meta-basalt showing; A) Crystals of andesine associated with chlorite of penninite type, meta-andesite, B) Carbonate patches associated with iron, meta-andesite, C) The plagioclase laths randomly oriented embedded in a matrix of altered pyroxene and quartz (intersertal texture), meta-basalt, D) Pyroxene including plagioclase showing sub-ophitic texture, meta-basalt, E) Phenocrysts of plagioclase partially sericitized, meta-dacite, F) Corroded quartz phenocrysts, meta-dacite.

IV. Geochemistry

4.1- Geochemistry of El Igla Metagabbros

The geochemical characterization of the El Igla metagabbros are carried out through the study of the chemical composition of seven selected samples (Fig. 1B). All the selected samples were analyzed for major, trace and rare earth element contents, and their CIPW norm values are computed (Table 1).

El Igla metagabbros can be divided into olivine metagabbros and normal metagabbros. The olivine metagabbros are represented by samples (G1, G3, G5 & G6), they have a low differentiation index (D.I=Q+ Or+ Ab [9], ranging from 20.89 to 32.63 with an average 26.92 (Table 2), this may indicate that, the original magma of these rocks was primitive and tholeitic in nature. The normal metagabbros are represented by samples (G2, G4, & G7), they have a very low differentiation index D.I=Q+ Or+ Ab [9], ranging from 14.75 to 28.85 with an average 23.70 (Table 2), this may indicate that, the original magma of these rocks was primitive and tholeitic to calc-alkaline in nature.

Table (1): Geochemical analysis of El Igla metagabbros, Central Eastern Desert, Egypt

le (1): Geo	ochemica	ii aiiaiysi		oxides (V		Central I	Lasterii D	esen, E		
S.No.	G1	G 2	G 3	G 4	G 5	G 6	G 7	Aver		
SiO ₂	49.73	46.91	49.31	48.00	46.95	46.43	48.22	47.94		
TiO ₂	0.74	0.61	0.89	0.45	0.41	0.56	0.38	0.58		
Al ₂ O ₃	16.6	19.0	17.14	18.29	19.05	18.10	16.2	17.77		
Fe ₂ O ₃	3.66	6.59	4.59	5.80	3.19	4.40	5.43	4.81		
FeO	4.3	4.75	3.79	3.18	4.30	4.05	3.10	3.92		
MnO	0.16	0.20	0.13	0.12	0.15	0.14	0.16	0.15		
MgO	8.52	4.70	6.87	7.54	8.22	9.0	8.11	7.57		
CaO	11.0	10.90	10.23	9.99	11.10	12.57	13.0	11.26		
	2.44		2.98	1.88	2.54		2.10	2.45		
Na ₂ O		2.60				2.63				
K ₂ O	1.10	1.0	1.10	1.77	1.12	0.45	0.47	1.00		
P ₂ O ₅	0.12	0.14	0.11	0.09	0.09	0.08	1.0	0.23		
LOI	1.37	2.44	2.0	2.34	2.54	1.44	1.50	1.95		
Total	99.74	99.84	99.14	99.45	99.66	99.85	99.67	-		
0	00	0.22		PW norn		0.0	1.04	0.25		
Qz	00	0.22	0.0	0.37	0.0	0.0	1.84	0.35		
Or	6.61	6.07	6.70	10.78	6.82	2.70	2.83	6.07		
Ab	20.96	22.56	25.93	16.36	19.76	18.19	10.08	19.12		
An	31.56	38.16	30.99	37.26	38.32	36.79	33.97	35.29		
ne	0.0	0.0	0.0	0.0	1.27	2.38	0.0	0.52		
Di (wo)	9.69	6.91	8.61	5.53	7.46	10.91	10.76	8.55		
Di (en)	7.33	5.09	6.84	4.67	5.45	8.51	8.98	6.70		
Di (fs)	1.36	1.14	0.77	0.13	1.29	1.18	0.39	0.89		
Hy (en)	9.70	6.98	8.61	14.74	0.0	0.0	11.67	7.39		
Hy (fs)	1.79	1.57	0.97	0.41	0.0	0.0	0.50	0.75		
Ol (fo)	3.24	0.0	1.57	0.0	10.99	10.05	0.0	3.69		
Ol (fa)	0.66	0.0	0.19	0.0	2.87	1.54	0.0	0.75		
Mt	5.39	9.81	6.85	8.66	4.76	6.48	8.02	7.14		
He	0.0	0.0	0.0	0.0	0.0	0.0	0.0	0		
II	1.43	1.19	1.74	0.88	0.80	1.08	0.74	1.12		
Ap	0.27	0.31	0.25	0.20	0.20	0.18	2.22	0.52		
D.I	27.57	28.85	32.63	27.51	26.58	20.89	14.75	25.54		
D,1	21.31			ements (20.07	14.75	23.3		
Ba	25	17	23	21	18	19	17	20		
Sr	30	22	29	30	17	16	19	23.29		
Rb	549	285	289	277	_	516	_	369.5		
					460					
Nb	246	203	189	201	188	236	214	211		
Y	49	33	50	18	43	26	19	34		
Zr	4	3	3	5	4	3	2	3.43		
Hf G	1.5	1.2	1.5	0.9	0.8	1.2	1.1	1.17		
Ga	26	25	26	21	24	20	22	23.43		
Co	14	14	12	12	11	14	13	12.86		
Ta	0.3	0.1	0.4	0.1	0.2	0.3	0.5	0.27		
Zn	25	22	58	52	24	32	29	34.57		
Ni	101	95	100	178	171	120	89	122		
Cr	341	148	167	364	580	139	301	291.4		
Cu	11	17	22	23	25	19	22	19.86		
Sc	36	45	44	29	32	36	30	36		
Au	1.14	0.12	0.13	1.12	0.17	0.12	1.15	0.56		
			1.1	1.1	1.7	1.3	1.09	1.22		
Ag 1.08 1.2 1.1 1.1 1.7 1.3 1.09 1.22 Rare earth elements (ppm)										
Ag		IX 2			\/					
	7.8				3.2	5.4	3.1	5.01		
La	7.8	3.3	8	4.3	3.2	5.4	3.1 23.2	5.01 21.4		
	7.8 25.9 2.11				3.2 18 0.22	5.4 20.1 0.30	23.2	5.01 21.4 1.10		

Sm	4.5	2.4	4.2	2.8	1.9	2	3.2	3
Eu	0.8	0.5	0.7	0.5	0.7	0.9	0.6	0.67
Gd	2.9	2.3	2.5	2.3	2.2	2.8	2.5	2.5
Tb	0.5	0.4	0.3	0.5	0.2	0.4	0.2	0.36
Dy	3.2	3.3	3.6	1.6	0.93	0.95	1.1	2.1
Ho	1.1	1.3	0.9	1	0.8	1.1	1.2	1.06
Er	1.4	2.4	1.9	1.7	0.47	0.60	1.1	1.37
Tm	0.6	0.4	0.5	0.3	0.4	0.5	0.3	0.43
Yb	2.9	1.9	2.8	2.7	2	2.8	1.9	2.43
Lu	0.1	0.2	0.2	0.1	0.3	0.1	0.2	0.17
∑LREE	62.11	43.22	56.33	49.95	40.72	45.8	50.4	49.79
∑HREE	9.8	9.9	10.2	7.9	5.1	6.5	6	7.91

Table (2): Some parameters and ratios of the studied metagabbros of El Igla area

	G1	G2	G3	G4	G5	G6	G7	Aver.
A/CNK	1.14	1.31	1.2	1.34	1.29	1.16	1.04	1.21
A/NK	4.69	5.28	4.26	5.01	5.2	5.88	6.3	5.23
Alkalies	3.54	3.60	4.08	3.65	3.66	3.08	2.57	3.45
FeOt	7.96	11.34	8.38	8.98	7.49	8.45	8.53	8.73
MgO+FeO ^t	16.48	16.04	15.25	16.52	15.71	17.45	16.64	16.3
FeO ^t /MgO	0.93	2.41	1.22	1.19	0.91	0.94	1.05	1.15
FeOt/(MgO+FeOt)	0.48	0.71	0.55	0.54	0.48	0.48	0.51	0.54
DI	27.57	28.85	32.63	27.51	26.58	20.89	14.75	25.54
Y/Nb	0.2	0.16	0.26	0.09	0.23	0.11	0.09	0.16
La/Yb	2.69	1.74	2.86	1.59	1.60	1.93	1.63	2.06
Dy/Yb	1.10	1.74	1.29	0.59	0.47	0.34	0.58	0.86
(La/Yb)n	1.94	1.25	2.06	1.14	1.15	1.39	1.17	1.44
(Dy/Yb)n	0.74	1.17	0.87	0.40	0.32	0.23	0.39	0.59

Generally, El Igla metagabbros have a medium contents of TiO_2 (0.38-0.89 wt%), and P_2O_5 (0.08-1.0wt %), K_2O (0.45-1.77wt %) and Na_2O (1.88-2.98 wt %), with modest variations in SiO_2 (46.43-49.73 wt %), while the Al_2O_3 , FeO, Fe₂O₃, and CaO have narrow ranges and high concentrations, these ranges are 16.2-19.05wt%, 3.10-4.75wt%, 3.19-6.59 wt%, and 9.99-12.57wt% respectively, except MgO has wide range is 4.70-9.0 wt %, (Table 1). El Igla metagabbros have very high total alkali concentrations, where Na_2O+K_2O values are between 2.57-4.08 wt% with the K_2O value much lower than Na_2O (Table 2).

The large ion Lithophile Elements (LILE) and the High Field Strength Elements (HFSE) have variable amounts in El Igla metagabbros, like Ba (17-25 ppm), Sr (16-30 ppm), Rb (211-549ppm), Zr (2-5 ppm), Nb (189-246 ppm), and Y (18-50 ppm) (Table 1). LIL elements (Ba, Rb, Sr, and K) are thus probable to have been remobilized during alteration and metamorphism to greenschist facies [10].

4.1.1- Geochemical Classification

The geochemical classification of the studied metagabbros is illustrated by two trends; the major oxides, and the normative minerals trend. They exhibit a slightly low degree of fractionation (DI. 14.75- 32.63 with average (25.54). On the (Na_2O+K_2O) vs. SiO_2 diagram [11]. El Igla metagabbros show that the all plotted samples are fall in the gabbro field (Fig. 8). On the Al_2O_3 -CaO-MgO diagram [12], this diagram has been used to differentiate between ultramafic and mafic cumulate rocks. Based on that the studied El Igla metagabbros, where they are classified as mafic cumulate rocks (Fig. 9). On the SiO_2 vs. K_2O diagram [13], El Igla metagabbros are classified largely as most medium-K rocks (Fig. 10).

4.1.2- Differentiation Index

The differentiation index (DI=Qz+Or+Ab), is calculated [9]. The differentiation index (DI) of el Igla metagabbros is plotted against some of the major oxides for illustrating the variation in the different oxides of the studied rocks (Fig. 11).

Figure (11) shows clearly that SiO₂, Na₂O, K₂O, Al₂O₃ and TiO₂ increase with increasing of the DI, while MgO, CaO and Fe₂O₃ show a marked decrease with increasing DI. It is easy to recognize on this diagram that a linear relationship is indicated no differences in the distribution of the elements argue for a single co-magmatic series.

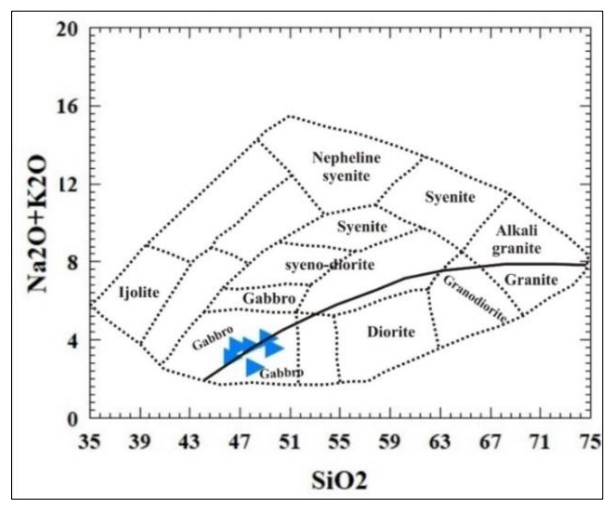


Fig. (8): Classification of the studied metagabbros, after (Cox et al., 1979)

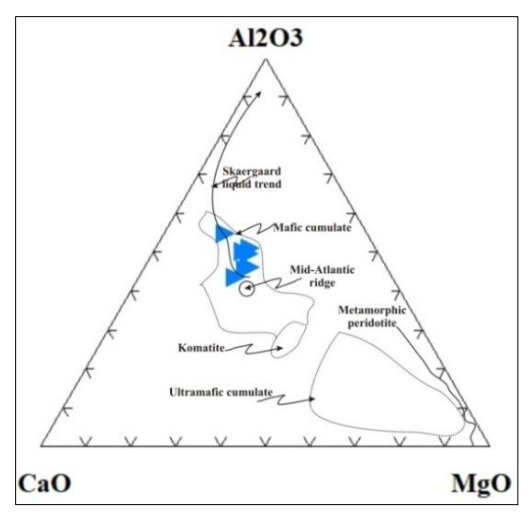


Fig. (9): Al₂O₃- CaO - MgO diagram (Colleman, 1977)

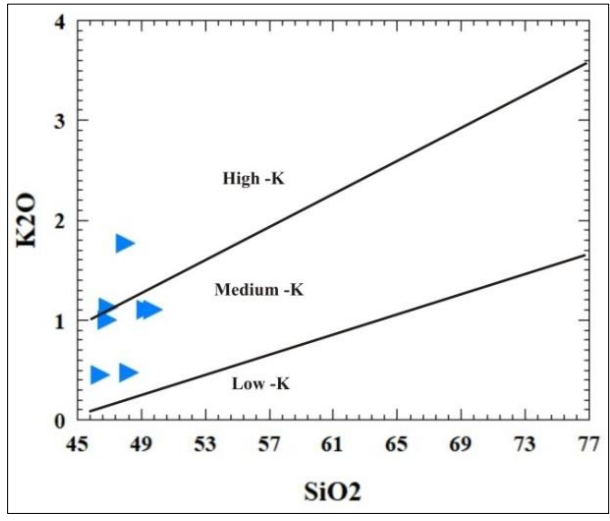


Fig. (10): SiO₂ vs. K₂O diagram (Le Maitre, 2002).

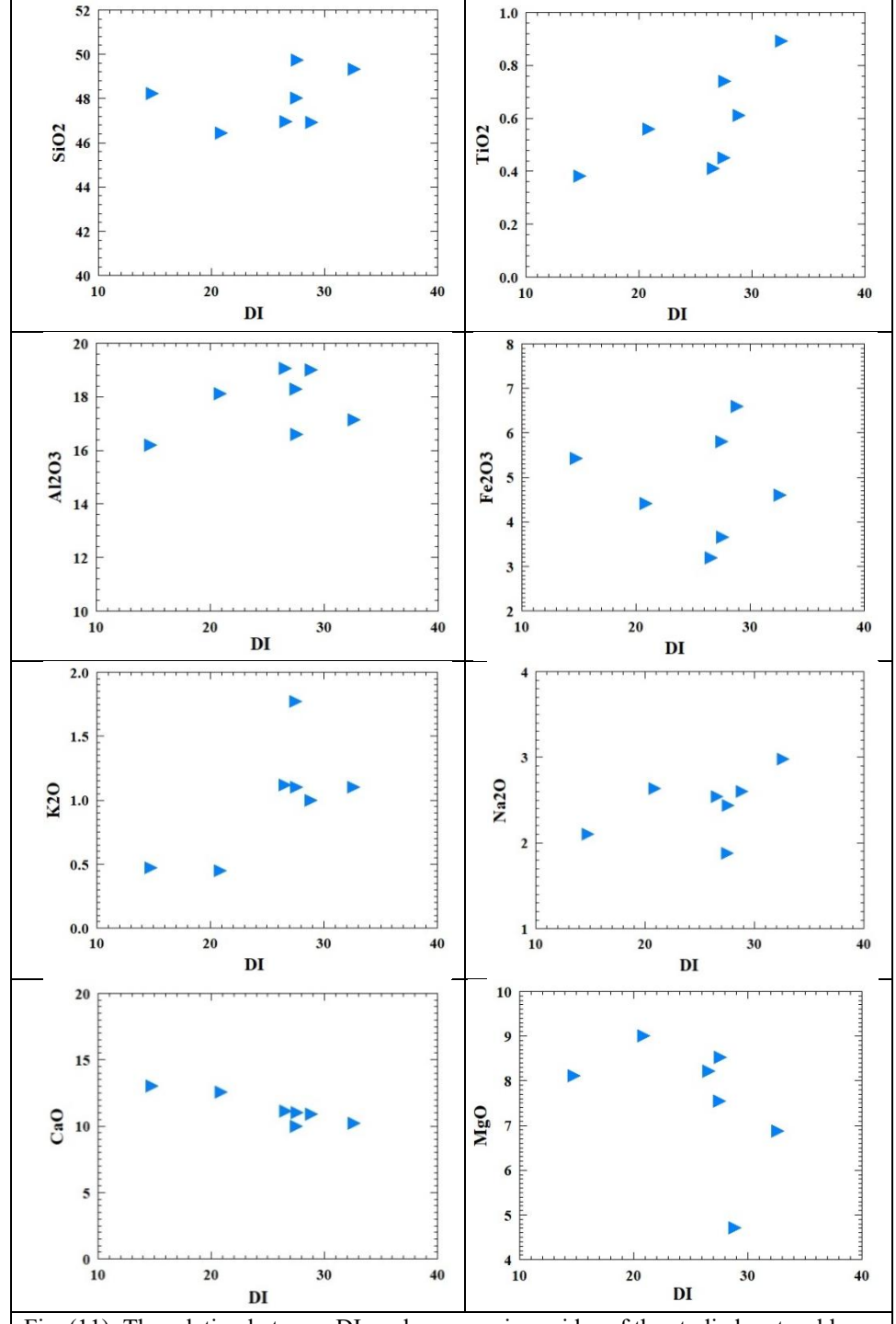


Fig. (11): The relation between DI. and some major oxides of the studied metagabbros. DI = Differentiation index (Qz+Or+Ab), after Thronton and Tuttle (1960).

4.1.3- Magma Type

On the *AFM* diagram suggested by Irvine, and Baragar, (1971) [14] to distinguish between tholeiitic and calc-alkaline series (Fig. 12), the plotted samples are located between calc-alkaline and theoiiltic field, due to their slightly enrichment in their alkalies.

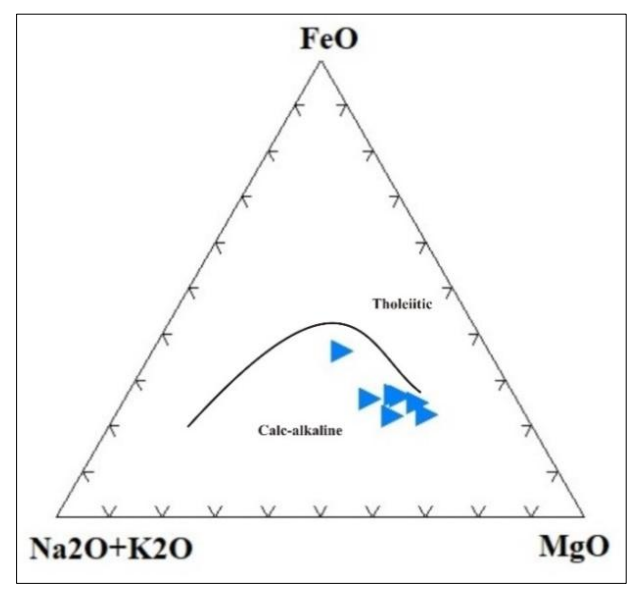


Fig. (12): Plots of the samples of the studied metagabbro on the AFM ternary diagram after (after T. N. Irvine, and W. R. A. Baragar)

4.1.4- Tectonic Setting

Major and trace elements, are used to show some light on the tectonic environments under which these rocks might have been formed. The *Ni vs. FeO/MgO* diagram [15] distinguishes between two different rock series MORB type and island-arc type. El Igla metagabbros fall in MORB type field (Fig. 13).

On the Al_2O_3 vs. TiO_2 diagram [16] shows El Igla metagabbros are located in the arc-related magma setting (Fig. 14).

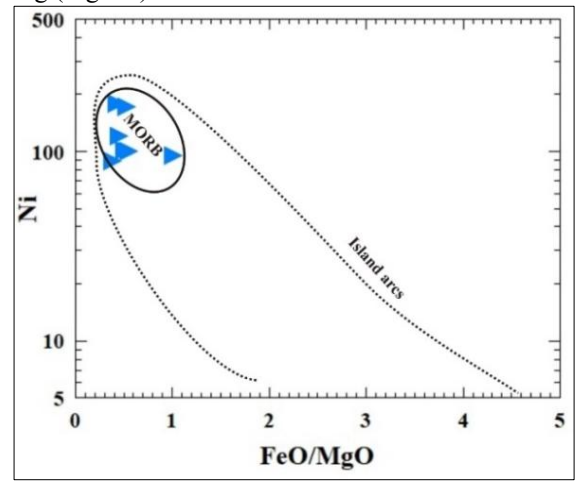


Fig. (13): Plots of Ni (ppm) vs. FeOt/MgO of El Igla metagabbros (after A. Miyashiro, and F. Shido, 1975)

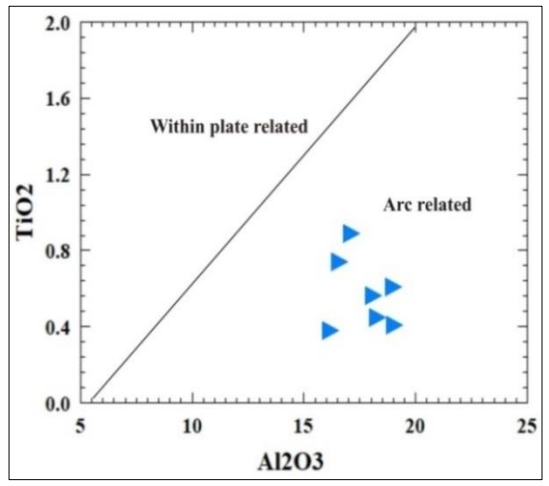


Fig. (14): Al₂O₃ vs. TiO₂, tectono-magmatic diagram of El Igla metagabbros (Muller and Groves, 1997)

The MgO vs. TiO_2 diagram [17] (Fig. 15), show that El Igla metagabbros are generally low MgO- low TiO_2 and very low TiO_2 Island Arc, calc-alkaline, indicating that they are generated in a subduction zone. El Igla metagabbros contain low- TiO_2 (0.38-0.89%) concentrations with average value (0.58%) and were probably derived from calc-alkaline magma.

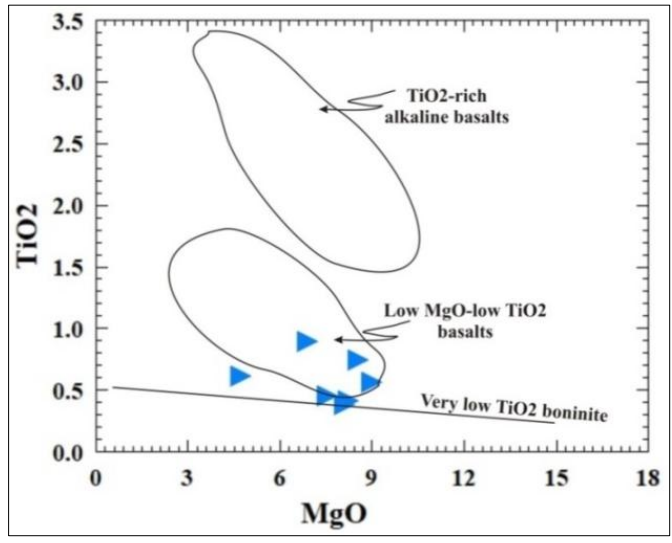


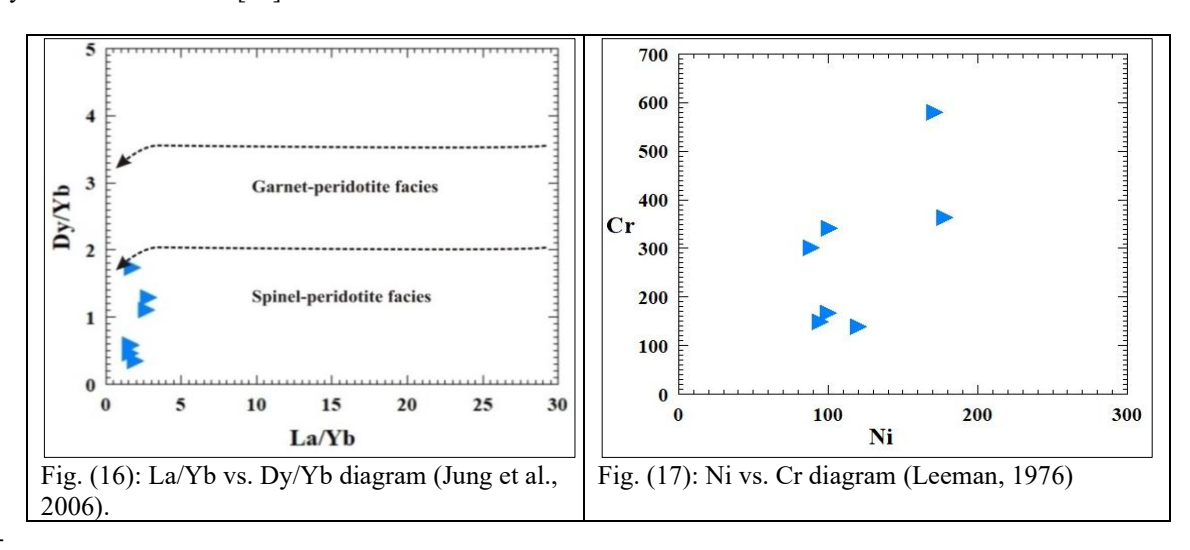
Fig. (15): MgO vs. TiO₂, tectono-magmatic diagram of El Igla metagabbros (Laurent and Hebert, 1989)

4.1.5- Petrogenesis

The REEs and HFSEs are immobile during the weathering and alteration processes. Magma origin is determined largely using the ratios and contents of HFSEs and LREEs [18]. In El Igla metagabbros, the La/Yb ratio (1.59-2.86) has a limited range, while the Dy/Yb ratio (0.34-1.74) is a wide range (Table 2 & Fig. 16), reflecting shallow source partial melting of spinel-peridotite [19]. The depletion of HFSEs likes Zr, Nb, Hf, and Pb refers to the separating of LILE such as Sr, Ba, Rb, and HFSEs during subducting slab dehydration [20]. Moreover, the depletion of HFS elements may result from fractionation and metamorphism processes [21]. El Igla metagabbros are formed as a result of partial melting of mantle spinel peridotite that has been metasomatized by fluids dehydrated from a subducted slab [22]. The Ni vs. Cr diagram [23] is significant in determining ferromagnesian mineral fractionation (Fig. 17). In El Igla metagabbros, based on positive trend between Ni-Cr and the absence of olivine in some samples, this indicates that it was derived from a previous fractionated origin or a melt that was slightly fractionated by removing olivine [24].

On the Chondrite-normalized rare earth elements (REE) pattern (Fig. 18), the REE in El Igla metagabbros are generally characterized by relatively parallel REE patterns with depletion of heavy rare earth elements (\(\sumeta\)HREE= 7.91) and enrichment in light rare earth elements (LREE=49.79) with [(La/Yb)n=1.17-2.06] (Table 1 & 2).

The spider diagram for primitive mantle (Fig. 19) exhibits depletion in some (HFSEs) like Zr and Hf with enrichment in others like Nb and Y, while, there are enrichments in (LILEs) like Rb, and depletion in Sr and Ba. Pearce et al. (1984) assumed that the eclectic depletion of Ba and Sr in comparison to Zr, and Y shown by calc-alkaline rocks [25].



DOI: 10.9790/0990-1306011029

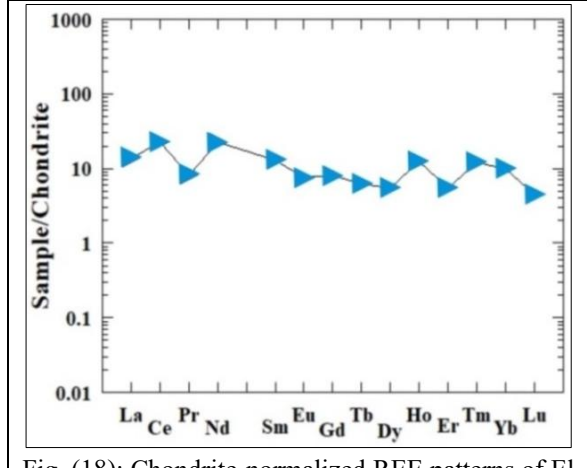


Fig. (18): Chondrite-normalized REE patterns of El Igla metagabbros (Sun and McDonough, 1989)

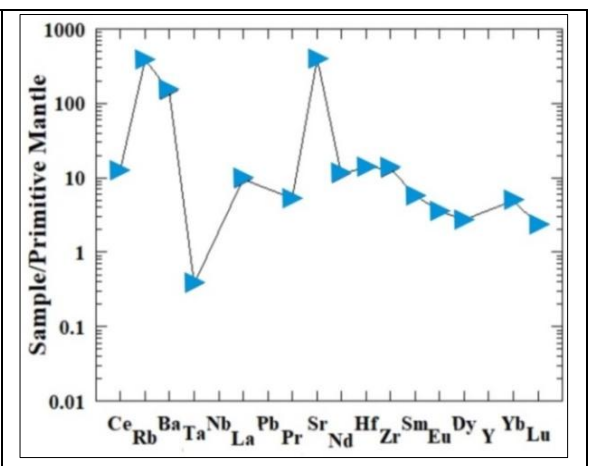


Fig. (19): Primitive mantle-normalized spider diagram of El Igla metagabbros of (Sun and McDonough, 1989).

4.2- Geochemistry of Metavolcanics

The geochemical characterization of the metavolcanic rocks at El Igla area is carried out through the study of the chemical composition of (9) selected samples representing, the outcrop of metavolcanic rocks at El Igla Iswied. All the selected samples were analyzed for their major, trace and rare earth element contents, as well as the CIPW norm values are computed (Table 3).

4.2.1- Major Element Characteristics

The studied samples (Table 3 & 4) showing high-alumina (Al_2O_3) contents ranging from 13 -15 wt% with an average 13.73, similar to those of calc-alkaline series rocks. Iron content (Fe₂O₃) seems to be relatively high ranging from 5.6- 11.2 wt%, with an average 8.97, and Fe₂O₃/MgO = <2 (1.53), this mean that high iron content reflect an abundant secondary opaque phase (magnetite). The studied samples show relative high abundance of CaO ranging from 5.4-13.4 wt% with an average 9.77, which may be related to the presence of epidote and non-intensive metamorphism [26]. There is abundance range of Na₂O (2.3 – 4.1 wt%), K₂O (0.15 – 0.97 wt%), and P₂O₅ (0.03–0.39 wt.%). The Cr abundances are generally high (105-496ppm)

Table (3): Major oxides, trace and rare earth elements analysis of El Igla Al Iswid metavolcanics, Central Eastern Desert, Egypt

	Major oxides (Wt%)										
S.No.	V1	V 2	V 3	V 4	V 5	V 6	V 7	V 8	V 9	Aver.	
SiO ₂	50.2	49.5	49.3	51	50	51.1	50.4	52.1	49.3	50.32	
TiO ₂	2.5	1.7	1.3	0.82	0.67	0.16	0.15	2.3	2.5	1.34	
Al_2O_3	14	14.1	12.5	13.4	13	13.7	15	14.9	13	13.73	
Fe ₂ O ₃	10	11.2	10.2	9.07	9.03	5.6	6.4	8	11.2	8.97	
FeO	3.10	3.25	3.39	3.08	3.10	3.15	3.55	3.12	3.18	3.21	
MnO	0.18	0.18	0.15	0.13	0.16	0.12	0.11	0.15	0.15	0.15	
MgO	4.8	4.2	6	6.7	7.1	8.8	8.3	6.8	5.2	6.43	
CaO	8.5	11	9.7	9.3	10.8	13.4	12.1	5.4	7.7	9.77	
Na ₂ O	3.3	3.7	4.1	3.5	2.5	2.3	2.4	3.8	3.8	3.27	
K ₂ O	0.97	0.29	0.21	0.15	0.33	0.34	0.45	0.72	0.85	0.48	
P ₂ O ₅	0.34	0.22	0.11	0.06	0.09	0.08	0.03	0.25	0.39	0.17	
L.O.I	1.9	0.51	2.9	2.8	3.2	1.3	1.1	1.7	2.6	2.0	
Total				100.0		100.0					
	99.79	99.85	99.86	1	99.98	5	99.99	99.24	99.87	-	
			•	C	IPW nor	m			•		
Qz	7.18	5.28	2.25	5.93	7.33	2.90	2.64	7.16	5.14	5.09	
Or	5.86	1.73	1.28	0.91	2.02	2.04	2.69	4.37	5.17	2.90	
Ab	28.49	31.48	35.74	30.43	21.83	19.68	20.51	32.93	33.02	28.23	
An	20.93	21.12	15.54	20.97	24.02	26.35	29.11	21.98	16.32	21.82	
Di (wo)	8.40	12.26	13.96	10.92	12.87	16.91	13.12	1.67	8.60	10.97	

Di (en)	7.24	10.57	12.04	9.41	11.09	14.04	10.48	1.44	7.42	9.30				
Di (fs)	0.0	0.0	0.0	0.0	0.0	0.71	0.62	0.0	0.0	0.15				
Hy (en)	5.02	0.0	3.43	7.82	7.25	8.24	10.14	15.99	5.95	7.09				
Hy (fs)	0.0	0.0	0.0	0.0	0.0	0.42	0.58	0.0	0.0	0.11				
Mt	3.40	6.17	7.88	8.20	8.85	8.22	9.38	3.97	3.58	6.63				
He	7.87	7.02	5.08	3.68	3.22	0.0	0.0	5.46	9.04	4.60				
Il	4.85	3.25	2.55	1.60	1.32	0.31	0.29	4.48	4.88	2.61				
Ap	0.76	0.48	0.25	0.13	0.20	0.18	0.07	0.56	0.88	0.39				
	Trace elements (ppm) Po 160 114 90 20 151 66 277 235 37 12067													
Ba	169	114	89	29	151	66	277	235	37	129.67				
Sr	239	230	161	88	235	116	300	380	355	233.78				
Rb	26	11	7	3.6	14	9	30	31	7.9	15.5				
Nb	17	5.8	2.4	1.6	9.3	4.7	17	21	11.9	10.08				
Y	46	35	27	25	45	13	36	40	69	37.33				
Zr	214	117	75	45	69	17	241	245	278	144.56				
Hf	18	10	11	9	8	5	19	18	20	13.11				
Ga	17.8	17.4	14.5	15.2	3.2	12.2	9.4	3.5	6.5	11.08				
Со	35.2	48.7	44.8	39	45	33	25	19	85	41.63				
Ta	1.5	0.6	0.5	0.3	0.5	0.06	1	0.7	1.25	0.71				
Zn	27 89	24	61 69	55	34	32	29	34	31	36.33				
Ni	155	145 496	220	119 412	125	107	28 105	38 123	111 363	92.33				
Cr Cu	26	58	66	54	478 27	406 65	24	28	26	306.44 41.56				
Pb	12	3.5	5.8	4.9	11	2.9	13	12	11	8.46				
V	270	315	335	241	265	119	145	159	115	218.22				
Sc	27	40	45	39	15	55	143	18	15	29.78				
Au	1.6	1.5	1.2	0.9	2	1.5	0.9	1	0.6	1.24				
Ag	0.6	1	0.9	1.1	0.8	1	0.9	1	0.7	0.89				
	0.0	_		Rare eart				-	0.7	0.07				
La	18.3	4.8	2.5	1.4	9.2	0.6	20	12	14	9.2				
Ce	44.1	17.3	9	5.2	1.4	19	30.1	102	105	37.01				
Pr	5.14	2.91	1.43	0.77	0.27	0.31	4.6	4.5	5.8	2.86				
Nd	25.8	14.7	9.90	5.40	4.80	6.90	19.3	18.9	13.7	13.27				
Sm	5.3	3.7	2.5	1.5	0.24	0.27	0.30	4	3.5	2.37				
Eu	1.22	1.40	0.98	0.55	0.15	0.19	0.15	1.98	2.65	1.03				
Gd	5.74	3.92	3.80	3.18	1.37	1.44	1.98	6	4.46	3.54				
Tb	1.10	0.91	0.70	0.45	0.09	0.10	0.08	1.89	0.97	0.70				
Dy	5.2	5.2	4.6	2.6	0.53	0.85	1	6.11	3.98	3.34				
Но	1.31	1.20	1.13	0.98	0.13	0.19	1.11	1.09	1.54	0.96				
Er	2.38	3.44	2.97	1.79	0.37	0.40	1.10	2.57	3.54	2.06				
Tm	0.51	0.50	0.48	0.36	0.08	0.09	0.09	0.48	0.55	0.35				
Yb	1.98	2.14	3.83	2.60	1.33	1.38	0.98	2.87	3	2.23				
Lu	0.47	0.48	0.49	0.27	0.16	0.19	0.39	0.30	0.55	0.37				
∑LRE	40	40 ==		4.5		••		149.3	149.1					
Е	105.6	48.73	30.11	18	17.43	28.71	76.43	8	1	69.28				
∑HRE	12.05	12.05	142	0.05	2.00	2.2	4.55	15.01	1413	10.03				
E	12.95	13.87	14.2	9.05	2.69	3.2	4.75	15.31	14.13	10.02				

Table (4): Some parameters and ratios of the studied metavolcanics at El Igla Al Iswid metavolcanics

	V1	V2	V3	V4	V5	V6	V7	V8	V9	Avion
	V I	V Z	V S	V 4	VS	VO	V /	vo	VY	Aver.
A/CNK	1.1	0.94	0.89	1.03	0.95	0.85	1	1.5	1.05	1.03
A/NK	3.28	3.53	2.9	3.67	4.59	5.19	5.26	3.3	2.8	3.84
Na ₂ O+K ₂ O										
Alkalis	4.27	3.99	4.31	3.65	2.83	2.64	2.85	4.52	4.65	3.75
Na ₂ O/K ₂ O	3.4	12.76	19.52	23.33	7.58	6.76	5.33	5.28	4.47	9.83
Fe ₂ O ₃ /MgO	2.08	2.67	1.7	1.3	1.27	0.64	0.77	1.18	2.15	1.53

FeO ^t	13.1	14.45	13.59	12.15	12.13	8.75	9.95	11.12	14.38	12.18
MgO+FeOt	17.9	18.65	19.59	18.85	19.23	17.55	18.25	17.92	19.58	18.61
FeO ^t /MgO	2.73	3.44	2.27	1.81	1.71	0.99	1.2	1.64	2.77	2.06
FeO ^t /										
(MgO+FeO)	1.66	1.94	1.45	1.24	1.19	0.73	0.84	1.12	1.72	1.32
DI	41.5									36.22
	3	38.49	39.27	37.27	31.18	24.62	25.84	44.46	43.33	
Y/Nb	2.71	6.03	11.25	15.63	4.84	2.77	2.12	1.91	5.8	5.90
Nb/Y	0.37	0.17	0.09	0.06	0.21	0.36	0.47	0.53	0.17	0.27
La/Ce	0.42	0.28	0.28	0.27	6.57	0.03	0.66	0.12	0.13	0.97
La/Y	0.39	0.14	0.09	0.06	0.2	0.05	0.56	0.3	0.2	0.22

4.2.2- Geochemical Classification

Silica (SiO₂) contents of El Igla metavolcanics confirm that they are dominantly andesite/basalt (SiO₂= 49.3-52.1wt %). On the Zr/TiO₂ vs. Nb/Y classification diagram (Fig. 20), the El Igla metavolcanics plot dominantly in the andesite/basalt with minor rhyolite/dacite field, whereas the two samples straddle the rhyolite/dacite boundary.

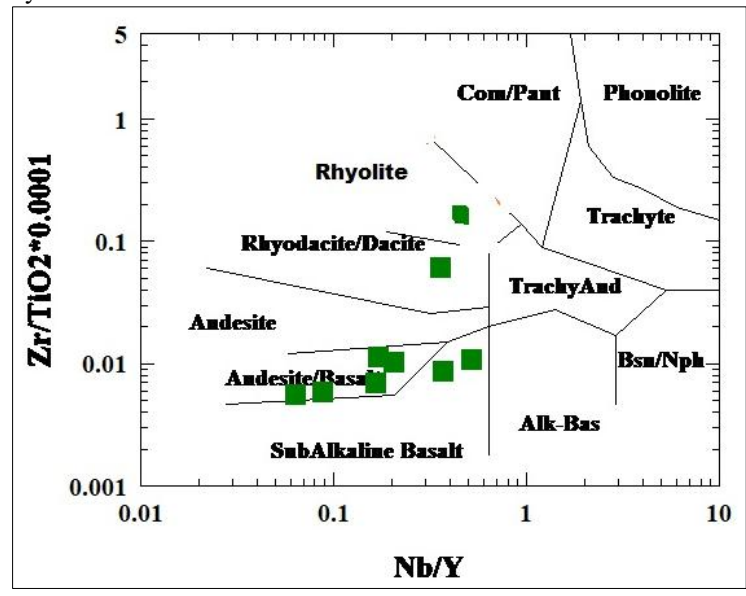


Fig. (20): Zr/TiO₂ vs. Nb/Y geochemical classifications of El Igla metavolcanics, (Winchester and Floyd, 1977).

4.2.3- Magma Type and Tectonic Setting

On the FeOt/MgO vs. SiO₂ diagram [27] of El Igla metavolcanics occupy the tholeitic field (Fig. 21). On the TiO₂ vs. SiO₂ diagram (Winchester and Max, 1984) and the P₂O₅/TiO₂ vs. MgO/CaO diagram [28], both discriminated diagrams showed El Igla metavolcanics as of magmatic origin, (Figs. 22 & 23).

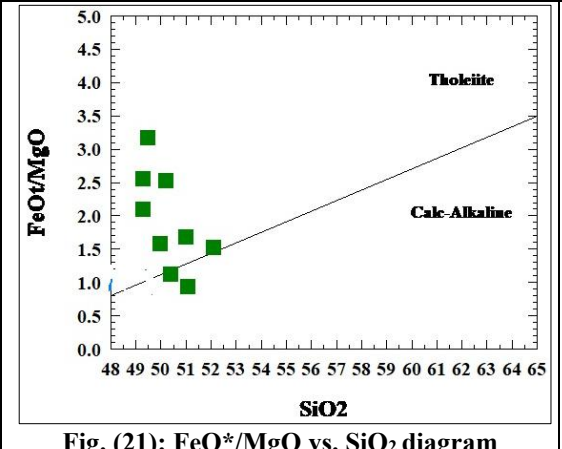


Fig. (21): FeO*/MgO vs. SiO₂ diagram (Miyashiro, 1974).

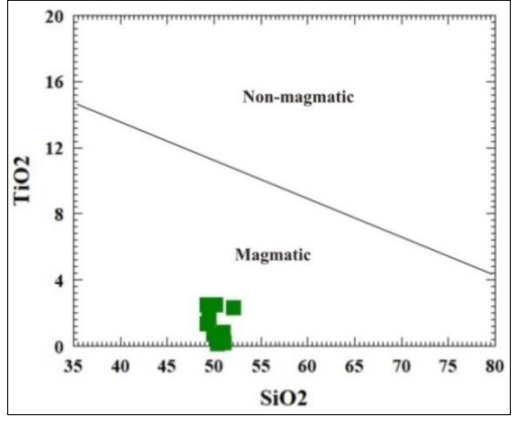
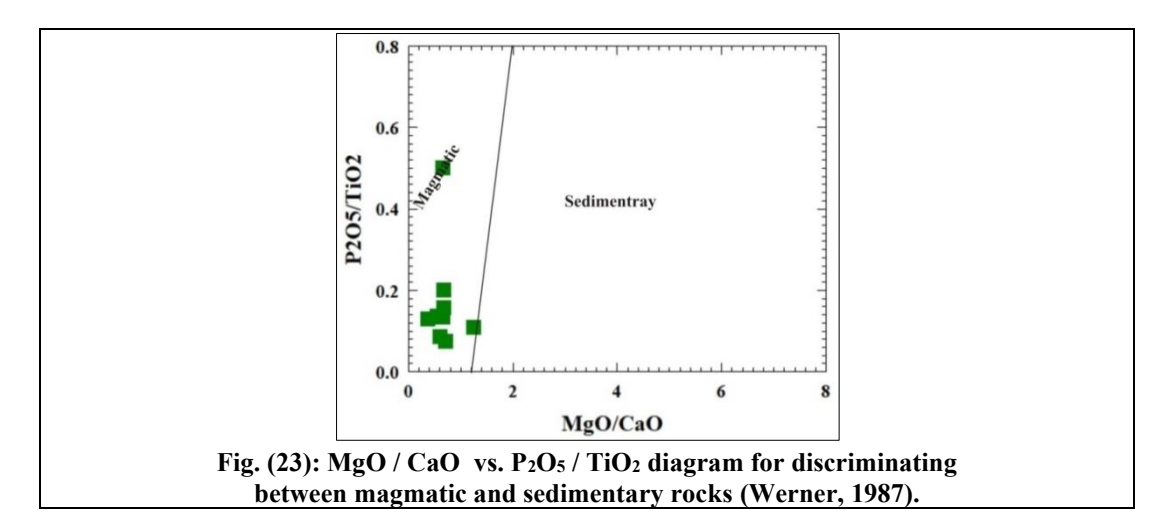


Fig. (22): SiO₂ vs. TiO₂ diagram between magmatic and non-magmatic rocks. (Winchester and Max, 1984),



4.2.4- Chemical Alteration and Element Mobility

The all selected samples of El Igla metavolcanics are altered to some extent due to the low-grade metamorphism and/or extensive deformations, reflected to the concentrations of the mobile elements and the moderate loss of ignition (LOI) values (Table 3). The present-day geochemical signature of metavolcanics may not be the same as the protoliths at the time of formation [29, 30]. Therefore, to illustrated the alteration effects of metamorphism and deformation, it can noticed element mobility through some major and trace elements against Silica (SiO₂ wt%). Harker variation diagrams [31], which show that compatible major oxides (MgO, TiO₂, FeOt, MnO, Al₂O₃), P₂O₅ and CaO (Fig. 24), have a normal, correlated and continuous differentiation trends, as they tend to decrease systematically with SiO₂ increases.

From Harker diagram (Fig. 25), Sr, Ni, Zr, Y, Ba and Cr demonstrate no clear variation with SiO₂, where they remain nearly unchanged, thus they were probably immobile during metamorphism and other alteration processes.

It is evident from figures (24 & 25), that, in spite of the low-grade metamorphism and deformation, some major and trace element signatures can be used for deciphering the original protoliths and tectonic environment.

Some major element concentrations span a wide compositional range of MgO (4.2-8.8 wt%) and MnO (0.11-0.18 wt%) with narrow compositional range of SiO_2 (49.3–52.1wt %), suggesting diverse protolith (Table 3).

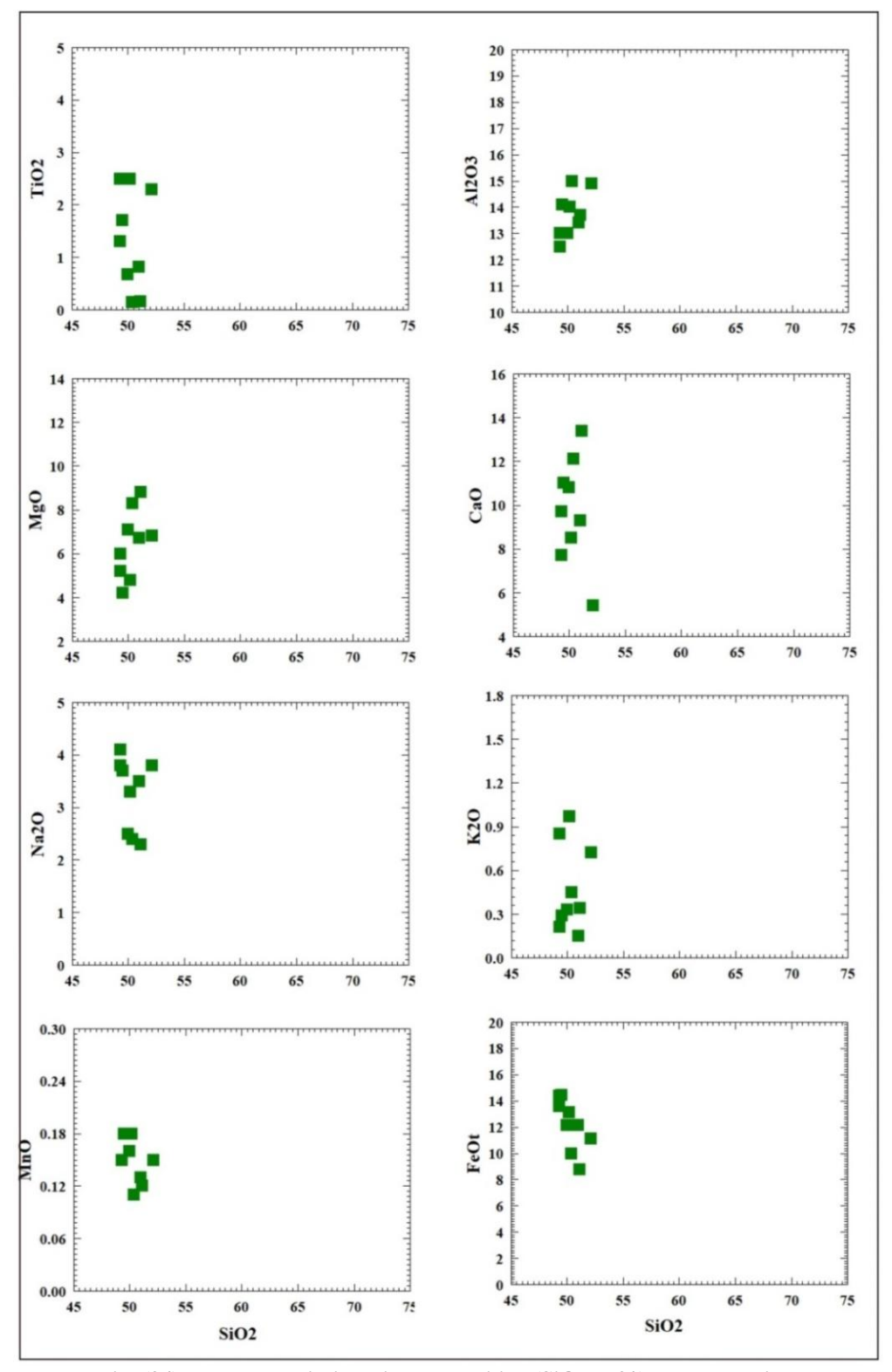


Fig. (24): Harker variation diagrams; silica (SiO₂ wt%) plotted against a range of major (wt%) of El Igla metavolcanics.

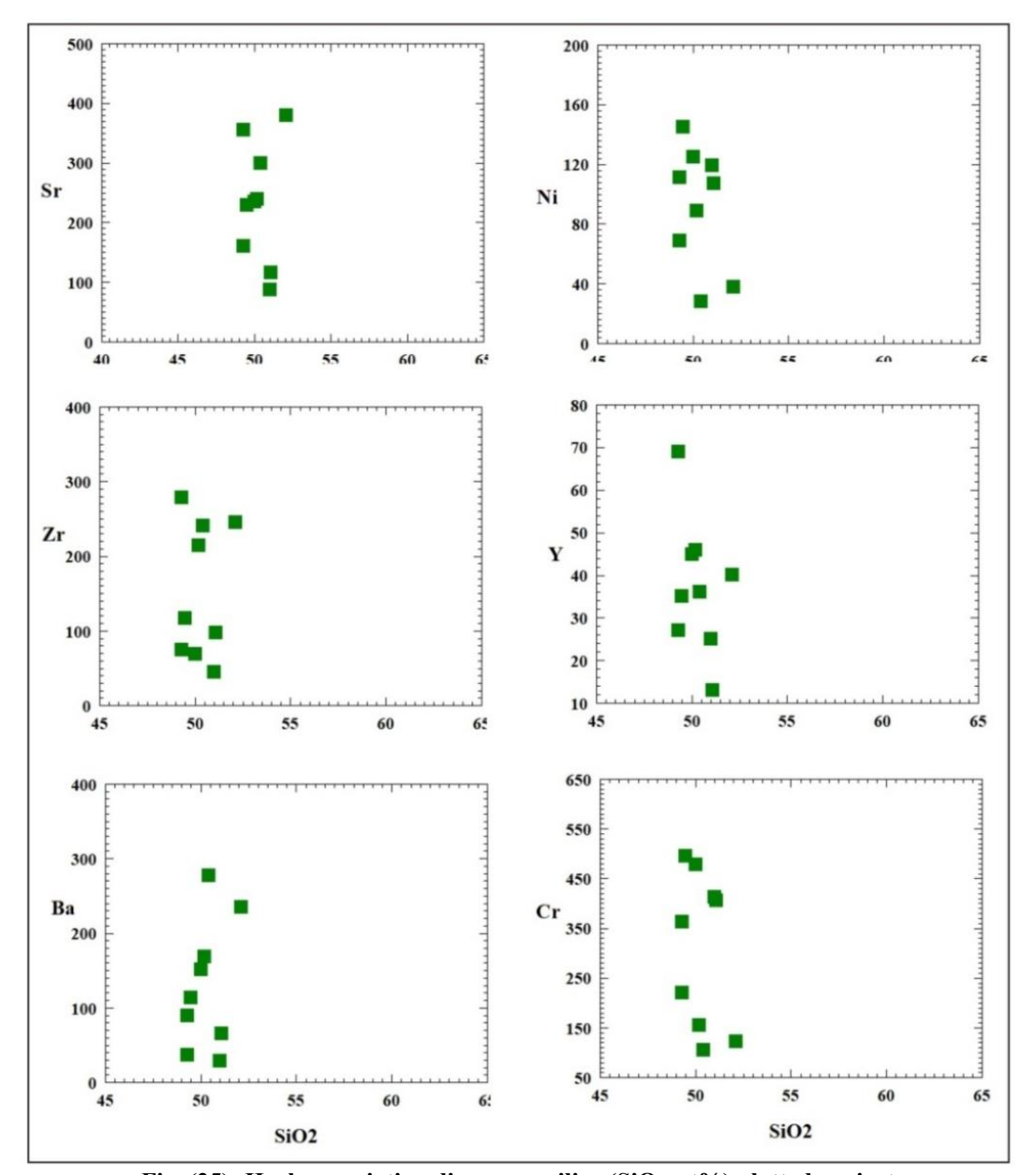


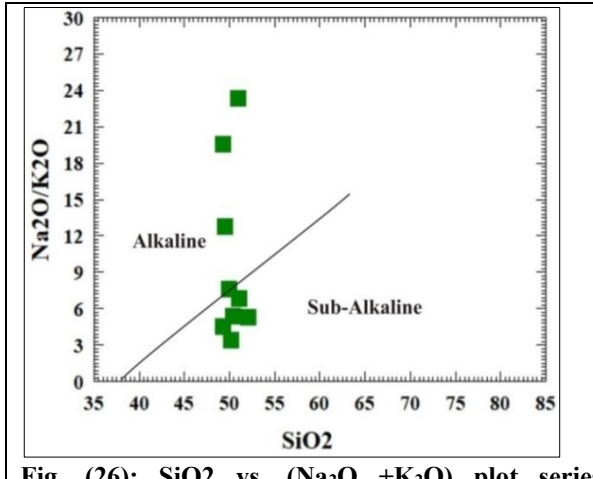
Fig. (25): Harker variation diagrams; silica (SiO₂ wt%) plotted against a range of trace elements (ppm) of El Igla metavolcanics.

4.2.5- Magma Characterization

The TiO_2 values are generally average (1.34), therefore they are in the range accepted in alkaline to calc-alkaline lavas [32, 33].

From table (5), the La/Sc ratios (0.03-6.57 with an average 0.97 ppm), the ratios of Y/Nb, and Nb/Y fall in the range between 1.91-15.63ppm with an average 5.90ppm and 0.06-0.53 ppm with an average 0.27ppm, respectively. The Nb/Y and La/Sc ratios are mostly < 1.0 and La/Y (0.05-0.56) with an average 0.22), implying possible approach to calc-alkaline and alkaline affinities [34].

On the SiO₂ vs. (Na₂O+K₂O) discrimination diagram [32], most plotted samples of El Igla metavolcanics fall in sub-alkaline to alkaline field (Fig. 26). K₂O vs. SiO₂ [35], which straddle the tholeitic and calc-alkaline boundaries indicate that the petrochemical composition of metavolcanic rocks fall within the calc-alkaline field (Fig. 27).



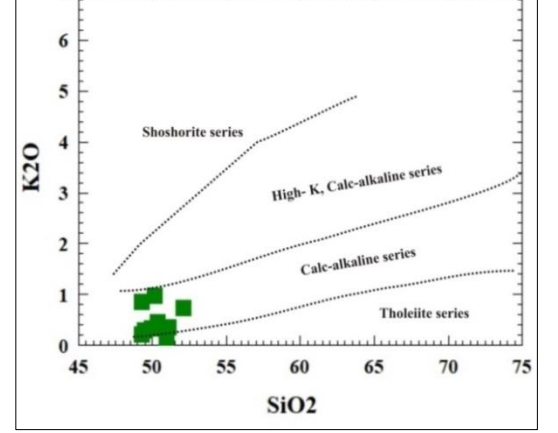


Fig. (26): SiO2 vs. (Na₂O +K₂O) plot series boundaries (after Irvine and Baragar, 1971)

Fig. (27): SiO₂ vs. K₂O, plot series boundaries (after Peccerillo and Taylor, 1976)

4.4.6- Geotectonic Setting

In the trace and rare earth elements content (Table 5), the abundances of Sr (88-380 ppm), Y (13-69 ppm) and La (0.6-18.3 ppm), Nb (1.6-21ppm), Ba (29-277 ppm), Ni (28- 145 ppm) and Zr (17- 278 ppm), is generally low-high, this feature suggesting the generation of these rocks arc-Island [36]. Plotting the immobile elements on the Zr vs. Y diagram [37], indicate that all samples discriminated as subduction-arc related rocks (Fig. 28).

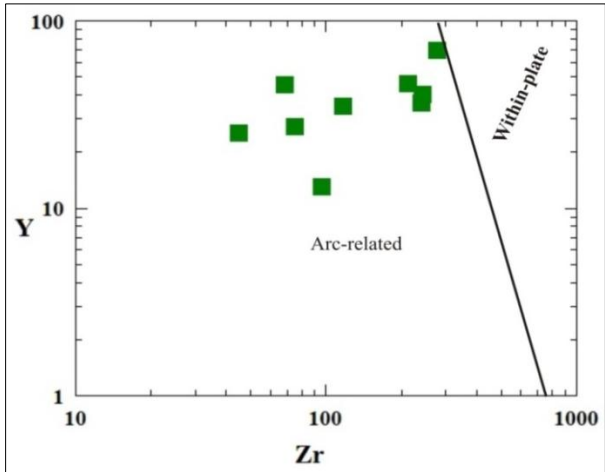


Fig. (28): Zr vs. Y Biaxial geochemical discrimination diagram indicating the subduction-arc features (Müller, et al., 2001)

In the chondrite-normalized REE pattern [38], all the analyzed El Igla metavolcanic samples display enrichment in fractionated light rare earth element (LREE: La, Ce, Pr, Nd and Sm) contents relative to heavy rare earth elements (HREE: Tb, Dy, Ho, Er, Tm, Yb and Lu) contents (Fig. 29). The Pattern is generally steep, moderately strong enrichment right-inclined type and lack Eu-anomalies similar to those from calc-alkaline to alkaline series. In the multi-element diagram normalized to primitive mantle [39], the data shows that El Igla metavolcanics possess a typical calc-alkaline island arc trace element patterns, enriched incompatible large ion lithophile elements (LILE: Sr & Ba) relative to high field strength elements (HFSE: Zr, Hf, Y, & Nb) contents, that show a negative Nb anomaly (Fig. 30).

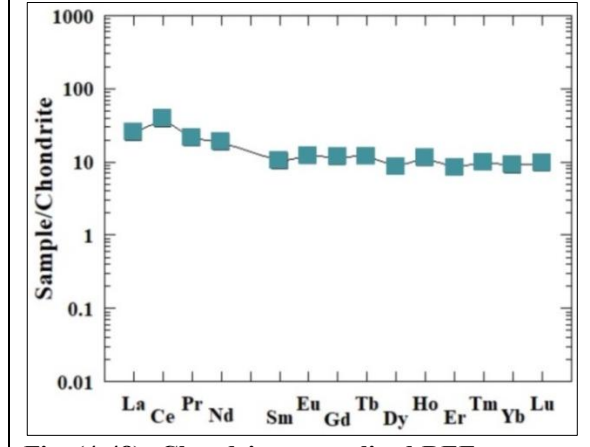


Fig. (4-48): Chondrite-normalized REE patterns of El Igla metavolcanic (Sun and McDonough, 1989)

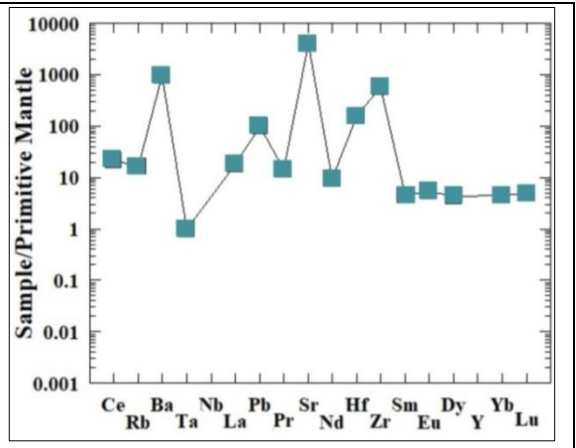


Fig. (4-49): Primitive mantle-normalized spider diagram of El Igla metavolcanic (McDonough and Sun, 1995).

V. Discussion and Conclusion

From field observations;

- ➤ El Igla metagabbros occurring as small to big outcrops, they are medium to coarse-grained and greenish grey to pale green in color. The ophiolitic metagabbros are found as small fragments and blocks associated with serpentinites forming low to moderately relief and composed of plagioclase, amphibole and pockets of hornblende.
- ➤ El Igla metavolcanics are exposed and comprise a heterogeneous of grey to green assemblages. They are coarse to medium grained and they are frequently interleaved with variably altered ultramafics (serpentinites) in the form of wedges and slices, with sharp tectonic contacts. El Igla metavolcanics are classified into meta-andesite, meta-basalt and meta-dacite rocks.

From petrographic view;

- El Igla metagabbros show ophitic to subophitic texture with calic pyroxenes and plagioclase as the major components. The alteration of El Igla metagabbros led to formation pyroxene, amphibole and actinolite.
- ➤ In El Iga metavolcanics, meta-andesite is composed essentially of plagioclase, hornblende and pseudomorphs chlorite. The accessory and secondary minerals are iron oxides, calcite, epidote and interstitial quartz. Meta-basalt is mainly composed of micro-phenocrysts of plagioclase, pyroxene and quartz set in fine-grained groundmass exhibiting intersertal texture. Meta-Dacite is composed predominantly of plagioclase, quartz and biotite. They have a fine grained aphanitic to porphyritic texture.

From geochemical view;

- ➤ In El Igla metagabbros, the original magma was primitive and tholeiitic to calc-alkaline in nature. They are fall in MORB type field and formed as a result of partial melting of mantle spinel peridotite that has been metasomatized by fluids dehydrated from a subducted slab. They are characterized by relatively parallel REE patterns with depletion of heavy rare earth elements (∑HREE= 7.91) and enrichment in light rare earth elements (LREE=49.79) with [(La/Yb)n=1.17-2.06].
- ➤ In El Igla metavolcanics, some major elements have wide compositional range of MgO (4.2-8.8 wt%) and MnO (0.11-0.18 wt%) with narrow compositional range of SiO₂ (49.3–52.1wt %), suggesting diverse protolith. The La/Sc ratios (0.03-6.57 with an average 0.97 ppm), the ratios of Y/Nb, and Nb/Y fall in the range between 1.91-15.63ppm with an average 5.90ppm and 0.06 − 0.53 ppm with an average 0.27ppm, respectively. The Nb/Y and La/Sc ratios are mostly < 1.0 and La/Y (0.05-0.56) with an average 0.22), implying possible approach to cale-alkaline and alkaline affinities with island are setting.

References

- [1]. Takla, M. A., Basta, E. Z. and Fauzi, E. (1981): Characterization of the older and Younger gabbros of Egypt. Delta. J. Sci. 279-314.
- [2]. Hassan, M. and Hashad, A. (1990): Precambrian of Egypt. In Said, R. (ed.) The Geology of Egypt. Balkema, Rotterdam, Brookfield, 201-245.
- [3]. Ali Bik, M.W. (1999a): Tectonic setting and petrogenesis of Sa'al el Rayan gabbroic rocks, south central Sinai, Egypt J Geol 43(1):131–146.
- [4]. Akaad, M.K. & Nowier, A.M. (1969): Lithostratigraphy of the Hammamat Um Seleimat District, Eastrn Desert, Egypt. Nature, 223, p. 248 285.
- [5]. El Ramly, M. F. (1972): A new geological map for the basement rocks in the Eastern and Southwestern Deserts of Egypt. Annals Geol. Surv. Egypt 2,1-18.

- [6]. Ali Bik, M. W., Abd El Rahim, S. H., and Wael Abdel Wahab (2013): Hornblende gabbros of Wadi Az Zarib area, Central Eastern Desert, Egypt: opaque mineralogy, geochemistry, tectonic setting, and petrogenesis, Arabian Journal of Geosciences, Volume 7, pages 4009–4027.
- [7]. Akaad, M. K. (1996): Rock succession of the basement. An introduction and assessent. Geol. Surv. Egypt, paper no. 71, p. 1-87.
- [8]. El Gaby, S., List, F. K. and Tehrani, R. (1988): Geology, evolution and metallogenesis of the Pan African belt in Egypt. In: El-Gaby, S. and R. O.Greiling (eds). The Pan African belt of northeast Africa and adjacent areas, Braun-Schweig (Vieweg), P. 17 68.
- [9]. Thoronton, C. p. and Tuttle, O. F. (1960): Chemistry of igneous rocks, Part I, differentiation index, Am. J. Sci, 258, 9, 664-684.
- [10]. Staudigel, H. (2003): Hydrothermal Alteration Processes in the Oceanic Crust, In Treatise on Geochemistry, edited by Holland, H.D., Turekian, K.K., Elsevier Pergamon. Oxford. pp. 511-535.
- [11]. Cox, K. G., Bell, J. D., and Pankhurst, R. J. (1979): The interpretation of igneous rocks. George. Allen and Unwin, London, pp. 468.
- [12]. Coleman, R. G. and Donato, M. M. (1979): Oceanic plagiogranite revisited: In Barker, F.(ed.), Trondhjemites, Dacites, and Related Rocks, Elsevier, Amsterdam, pp.49-168.
- [13]. Le Maitre, R.W. (2002): Igneous Rocks: A Classification and Glossary of Terms. Cambridge University Press, Cambridge, and New York.
- [14]. Irvine, T. N., and Baragar, W. R. A. (1971): A guide to chemical classification of the common volcanic rocks. Canada: J. Earth Sci., Vol. 8, pp. 523-548.
- [15]. **Miyashiro, A. and Shido, F. (1975):** Tholeitic and calc-alkaline series in relation to the behavior of titanium, vanadium, chromium and nickel. Am. J. Sci., 275, 265-277.
- [16]. Muller, D. and Groves, D. (1997): Potassic Igneous Rocks and Associated Gold-Copper Mineralization. Springer-Verlag, Berlin, Heidelberg
- [17]. **Laurent, R. and Heberi, R. (1989):** The Volcanic and Intrusive Rocks of the Quebec Appalachian Ophiolites (Canada) and their Island Arc Setting. Chemical Geology 77: 287-302.
- [18]. Zhang, B. L., Lv, G. X., Su, J., Shen, X. L., Liu, R. L., Liu, J. G., Hai, L. F., Zhang, G. L. (2015): A Study of the Tectono-Lithofacies Mineralization Regularities of the Gejiu tin Polymetallic Orefield, Yunnan, and Prospecting in its Western Part. Earth Science Frontiers 22: 078-087.
- [19]. Thirlwall, M. F., Upton, B. G. J., Jenkins, C. (1994): Interaction between Continental Lithosphere and the Iceland Plume: Sr–Nd–Pb Isotope Chemistry of Tertiary Basalts, NE Greenland. Journal of Petrology 35: 839-897.
- [20]. Shawna, M., Leatherdale, Maxeiner, R. O., Ansdell, K. M. (2003): Petrography and Geochemistry of Love Lake Lecogabbro, Swan River Complex, Peter Lake Domain, Northern Jour. Saskatchewan, Saskatchewan Geological Survey 2: 1-17.
- [21]. **John, T., Scherer, E.E., Haase, K., Schenk, V. (2004):** Trace element fractionation during fluid-induced eclogitization in a subducting slab: trace element and Lu–Hf–Sm–Nd isotope systematics. Earth and Planetary Science Letters 227, 441–456.
- [22]. Wang, J. P., Wang, X., Liu, J. J., Liu, Z.J., Zhai, D. G., Wang, Y.H. (2019): Geology, Geochemistry, and Geochronology of Gabbro from the Haoyaoerhudong Gold Deposit, Northern Margin of the North China Craton. Minerals 9(63): 1-18.
- [23]. Leeman, W. P. (1976): Petrogenesis of Mckinney (Snake River) Olivine Tholeite in the Light of Rare-Earth Elements and Cr/Ni Distributions. Geological Society of America Bulletin 87: 1582-1586.
- [24]. Wilson, S. A. (2001): The Geochemical Analysis of Siluro-Devonian Mafic Dikes in the 15' Woodsville Quadrangle, East-Central Vermont, Senior Thesis, Middlebury College, Middlebury, Vermont.
- [25]. Pearce, J. A.; Harris, N. B. W.; and Tindle, A. G. (1984): Trace element discrimination diagrams for the tectonic interpretation of granitic rocks. Jour. Petro. 25, 958-983.
- [26]. **Jakes, P. and White A. J. R. (1972):** Major trace element abundances in volcanic rocks of orogenic areas. Geol. Soc. Am. Bull. 83: 29–40.
- [27]. Miyashiro, A. (1974): Volcanic rocks series in island arc and active continental margins. Am. Jour. Sci., 274. p.321-355.
- [28]. Werner, C. D. (1987): Saxonium granulites: a contribution to the geochemical diagnosis of original rocks in high-metamorphism complexes, Gerlands Beitraege zur Geophysik, 96; 271-290.
- [29]. Irvine, I. J. and Green. H. (1976): Geochemistry and Petrogenesis of the newer bashs of Victoria and South Australia. Journal of Geol. Soc. of Australia. 23 (2): 45.
- [30]. Alfred, J. E. and Michael, G. D. (1989): Discrimination between altered and unaltered rocks at the Connemarra and Kathleen Au deposits, western Australia. Jou. Geochem. Explor. 31: 237-252.
- [31]. Harker, A. (1909): The natural history of igneous rocks. Macmillan, New York.
- [32]. Irvine, T. N. and Barager, W. R. A. (1971): A guide to the chemical classification of the common volcanic rocks. Canadian Journal of Earth Science. 8: 523-548.
- [33]. **Pearce, J. A. and Conn, J. R. (1973):** "Tectonic setting of basic volcanic rocks determined using trace element analyses". Earth Planet Sci. Lett: V. 19, 289-300.
- [34]. Garcia, M. O. (1978): Criteria for identification of ancient volcanic arc. Earth and Planetary Science Letters. 14: 147–165.
- [35]. **Peccerillo, A. and Taylor S. R. (1976):** Geochemistry of Eocene calcalkaline rocks from Kastamonu area northern Turkey. Contributions to Mineralogy and Petrology. 68: 63-81.
- [36]. **Pearce, J. A., and Gale, G. H. (1977):** Identification of ore-deposition environment from trace element geochemistry of associated igneous host rocks: Geological Society of London Special Publication, Vol. 7, pp. 14-24.
- [37]. Müller, D., Franz, L., Herzig, P. M. and Hunt, S. (2001): Potassic igneous rocks from the vicinity of epithermal gold mineralization, Lihir Island, Papua New Guinea. Lithos. 75: 163-186.
- [38]. Sun, S.S., McDonough, W.F. (1989): Chemical and isotopic systematics of oceanic basalts: implications for mantle composition and processes. In: Saunders, A.D., Norry, M.J. (Eds.), Magmatism in ocean basins. J. Geol. Soc. Lond., Special Publications 42, pp. 313–345.
- [39]. McDonough, W. F. and Sun, S. S. (1995): The composition of the earth. Chemical Geology. 120: 223-253.